CrystEngComm

ROYAL SOCIETY OF CHEMISTRY

PAPER

View Article Online
View Journal | View Issue

Check for updates

Cite this: *CrystEngComm*, 2021, **23**, 5624

Study of flux crystal growth peculiarities, structure and Raman spectra of double $(Mn,Ni)_3BO_5$ and triple $(Mn,Ni,Cu)_3BO_5$ oxyborates with ludwigite structure†

Evgeniya Moshkina, *[a] Asya Bovina,[a] Maxim Molokeev, [abc] Alexander Krylov, [a] Alexander Shabanov,[ad] Artem Chernyshov[ae] and Svetlana Sofronova[a]

Received 7th June 2021,
Accepted 26th June 2021

DOI: 10.1039/d1ce00750e

rsc.li/crystengcomm

Crystallization of heterovalent double $(Mn,Ni)_3BO_5$ and triple $(Mn,Ni,Cu)_3BO_5$ oxyborates with the ludwigite structure is studied in fluxes based on $Bi_2Mo_3O_{12}$ diluted with Na_2CO_3 or Li_2CO_3 carbonates. Single crystals of five $(Mn,Ni)_3BO_5$ and three $(Mn,Ni,Cu)_3BO_5$ compounds with different cation ratios are obtained. The ion concentration is determined from the analysis of the lattice parameters by powder and single crystal XRD. The comparative analysis of the polarized Raman spectra of double and triple ludwigites is presented. The actual high nickel and small copper concentrations in the crystals are discussed. The hierarchy of chemical bonds in the fluxes used in addition to the approach involving stabilization of the manganese valence state using solvent components is estimated.

1. Introduction

The creation of new perspective materials is one of the main aspects of successful science and technology development. To date, several scientific teams have dealt with the synthesis and properties of ludwigite type compounds.[1–7] The ludwigite structure (Fig. 1) is quasi-two-dimensional and includes zigzag walls constructed from octahedra MO_6 with heterovalent cations M^{x+} (x = 2/3, 2/4, 2/5, 2/3/4). The study of ludwigite is complicated by the small size of its crystals. The quasi-two-dimensional arrangement of structural elements is the cause of a considerable growth anisotropy.[5] Therefore, the crystals have the shape of a prism with the longitudinal size being an order of magnitude larger than other sizes. This imposes significant restrictions on choosing the growth technique.

Thus, a ludwigite crystal often does not have a size sufficient for the orientational measurements.[3,4] The flux method is one of the most promising methods for growing large crystals.[5–7] The most frequently used solvents for the synthesis of ludwigites are boron oxide B_2O_3 (ref. 7 and 8) or borax $Na_2B_4O_7$.[6,9] The size of single crystal samples is highly dependent on the cation type. For instance, a single crystal cross-section of some composition of copper ludwigites can amount to a millimeter,[5,10,11] but the longitudinal size of many Co-, Ni-, Fe-containing ludwigites can be as small as a fraction of a millimeter.[3,6,8]

Another approach uses the mixture $Bi_2Mo_3O_{12}$–B_2O_3 diluted in alkaline metal carbonates, and it results in

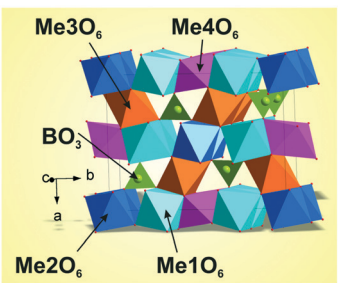

Fig. 1 Ludwigite structure. The structural elements are denoted by the following colors: cyan – $Me1O_6$ octahedra, blue – $Me2O_6$ octahedra, orange – $Me3O_6$ octahedra, pink – $Me4O_6$ octahedra, and green – $[BO_3]^{-6}$ triangles. Me1, Me2, Me3, and Me4 are the non-equivalent metal cation positions corresponding to 4*g*, 2*a*, 4*h*, and 2*d*, respectively (depending on the compositions of heterovalent cations (Ni^{2+}, Cu^{2+}, Mn^{2+}, Mn^{3+}, Mn^{4+}) which are distributed over these positions with different probabilities and different weights).

[a] *Kirensky Institute of Physics, 660036 Krasnoyarsk, Russia. E-mail: ekoles@iph.krasn.ru*
[b] *Siberian Federal University, Krasnoyarsk, 660041, Russia*
[c] *Research and Development Department, Kemerovo State University, Kemerovo, 650000, Russia*
[d] *Federal Research Center "Krasnoyarsk Science Center of the Siberian Branch of the Russian Academy of Sciences", 660036 Krasnoyarsk, Russia*
[e] *Reshetnev Siberian State University of Science and Technology, 660037 Krasnoyarsk, Russia*

† Electronic supplementary information (ESI) available. CCDC 2087975–2087977. For ESI and crystallographic data in CIF or other electronic format see DOI: 10.1039/d1ce00750e

successfully obtaining Cu_2GaBO_5,[5,12] Cu_2FeBO_5 (ref. 12) and solid solutions of ludwigites, for example, $(Mn,Ni)_3BO_5$,[13–16] $(Mn,Cu)_3BO_5$,[10,11] and $(Mn,Co)_3BO_5$.[17]

$Mn_{3-x}Ni_xBO_5$ ludwigites were obtained with a wide range of x values using the flux system based on bismuth trimolybdate.[13–15] These compounds demonstrate many interesting physical properties and high sensitivity even to small changes in the composition, such as strong magnetization anisotropy, and high temperatures of magnetic phase transitions. $Ni_{1.5}Mn_{1.5}BO_5$ shows large magnetic hysteresis providing field cooled cooling (FCC) and field cooled warming (FCW) below the phase transition temperature.[16] $Ni_{1.8}Mn_{1.2}BO_5$ has magnetization reversal,[13] and $Ni_{2.25}Mn_{0.75}BO_5$ exhibits exchange bias.[15]

In contrast, $Mn_{3-x}Cu_xBO_5$ was obtained with a narrow range of x values in the flux (the compound composition is taken as the ratio of the initial flux components).[10,11,16] The crystal structure of these samples is quite different from orthorhombic ludwigites ($(Mn,Ni)_3BO_5$, $(Mn,Co)_3BO_5$)[10,11] and other Cu-containing monoclinic ludwigites (Cu_2MeBO_5, where Me = Al, Ga, Fe).[5,7,12,16] Apparently, this is due to the presence of two Jahn–Teller cations, namely Cu^{2+} and Mn^{3+}. NiO and Ni_2O_3 have low solubility in usual flux systems, including $Bi_2Mo_3O_{12}$–B_2O_3, which results in low concentrations of crystal-forming components.[18,19] In contrast to NiO and Ni_2O_3, CuO oxide is characterized by high solubility in $Bi_2Mo_3O_{12}$–B_2O_3.

Cu_2MnBO_5 ludwigites are ferrimagnets with a relatively high magnetic moment, their temperatures of magnetic ordering being about 90 K. Similar to $Ni_{1.5}Mn_{1.5}BO_5$, some $(Mn,Cu)_3BO_5$ compounds also show magnetic hysteresis with FCC and FCW below T_c. In general, the magnetic anisotropy of $(Mn,Ni)_3BO_5$ and $(Mn,Cu)_3BO_5$ ludwigites is very different. Cu_2MnBO_5 was the first heterometallic ludwigite with an experimentally determined magnetic structure. It includes two non-collinear magnetic subsystems oriented to each other at an angle of ~60°. Magnetic moments inside each subsystem are directed antiferromagnetically. In Cu_2MnBO_5, the rotational magnetocaloric effect[20] and anomalous dependence of magnetostriction under the applied magnetic field $H||a$ (ref. 21) were detected.

The problem of growing and studying triple $(Mn,Ni,Cu)_3BO_5$ ludwigites is of high importance both from the viewpoint of creating compounds with new properties formed as a result of substitutions in the bivalent system and from the viewpoint of the growth process, *i.e.* investigation of the chemical bond competition in the multicomponent flux in the simultaneous presence of two (Ni,Cu) bivalent cation types.

2. Experimental conditions

2.1 Synthesis conditions

Single crystals of double $(Mn,Ni)_3BO_5$ and triple $(Mn,Ni,Cu)_3BO_5$ ludwigites were obtained by a flux technique. The crystal growth was carried out at normal pressure in air using a resistance furnace equipped with silicon carbide heaters. The used temperature range was T = 750 ÷ 1100 °C. Fluxes for each composition were prepared in a platinum crucible (V = 100 cm^3) at the temperature T = 1100 °C by sequential melting of the flux system components in the following order: first, the Bi_2O_3–MoO_3–B_2O_3 powder mixture was melted, then Na_2CO_3 (Li_2CO_3) was added in portions, and finally, Ni_2O_3 (CuO) and Mn_2O_3 were also added in portions. Under heating, there was the transition of $Ni^{3+}{}_2O_3$ and $Mn^{3+}{}_2O_3$ oxides to $Ni^{3+}{}_2Ni^{2+}O_4$ and $Mn^{3+}{}_2Mn^{2+}O_4$ accompanied by oxygen loss. Under heating of carbonate Na_2CO_3, the decomposition occurred with the release of CO_2, corresponding to the chemical reaction $Na_2CO_3 \rightarrow Na_2O + CO_2\uparrow$ (the same for Li_2CO_3). Due to this, in flux system (1) Na_2O (Li_2O) oxide was used instead of Na_2CO_3 (Li_2CO_3). The prepared fluxes were homogenized for 3 hours at the melting temperature T = 1100 °C.

The crystal formation in the prepared fluxes was estimated, and the sequence of high-temperature crystallizing phases was studied. The fluxes were investigated in a wide temperature range. After the homogenization stage, the temperature in the furnace was reduced rapidly at a cooling rate of 100 °C h^{-1} down to the estimation temperature T in the range of 850 ÷ 950 °C. The temperature step of probing was ΔT = 10 °C. After 24 h the crucible was removed from the furnace, the flux was poured out, and the crystal formation was estimated.

2.2 Powder X-ray diffraction

The powder diffraction data of the synthesized samples for the Rietveld analysis were collected at room temperature with a Bruker D8 ADVANCE powder diffractometer (Cu-Kα radiation) and a linear VANTEC detector. The step size of 2θ was 0.016°, and the counting time was 1 s per step.

2.3 Single crystal X-ray diffraction

The crystal structure of the single crystal samples was investigated by the X-ray diffraction method at room temperature using a SMART APEX II diffractometer (Mo K_α, λ = 0.7106 Å). The structures were solved by direct methods using the package SHELXS and refined in the anisotropic approach for all the atoms using the SHELXL program.[22] The structure test for the presence of missing symmetry elements and possible voids was performed using the program PLATON.[23] The DIAMOND program was used for plotting the crystal structure.[24]

2.4 EDX spectroscopy

Energy-dispersive X-ray spectroscopy (EDX) was performed. The crystal samples were examined on a Hitachi TM-4000 Plus desktop scanning electron microscope at an accelerating voltage of 20 kV. Elemental mapping was performed using a Bruker XFlash 630Hc X-ray detector. The spectra were analyzed using the Quantax 70 program.

2.5 Raman spectroscopy

The Raman spectra in the backscattering geometry were recorded with a Horiba Jobin Yvon T64000 triple spectrometer equipped with a liquid nitrogen-cooled charge-coupled device detection system in the subtractive dispersion mode. The single crystal of ludwigite was oriented relative to the excitation laser beam, with the *z*-axis coinciding with the *c* crystallographic axis directed along the needle (Fig. 5). The Spectra-Physics Excelsior continuous-wave solid-state laser with λ = 532 nm and power of 0.5 mW on a sample was used as an excitation light source. The microscope system based on an Olympus BX-41 microscope (with an Olympus MPlan 100× objective lens f = 0.8 mm with numerical aperture N.A. = 0.9) was used to measure the polarized Raman spectra of the single crystal. The laser beam was focused into a spot with a diameter of 2 μm.

3. Crystal growth

3.1 Flux growth of double $Mn_{3-x}Ni_xBO_5$ ludwigites

Crystallization of $Mn_{3-x}Ni_xBO_5$ ludwigites was studied in two flux systems based on $Bi_2Mo_3O_{12}$–B_2O_3 diluted with Na_2CO_3 or Li_2CO_3 carbonates. Using the Na-containing flux system, compounds of three compositions (x = 2.25, 2.17, 0.5) were grown. Using the Li-containing flux system, compounds of two compositions (x = 1.5, 1.8) were grown. The use of two carbonates enables us to study the influence of the solvent on the crystallization of Mn-heterovalent compounds.[22]

3.1.1 Na_2CO_3 – containing flux system. The initial Na-containing flux system for growing $Mn_{3-x}Ni_xBO_5$ ludwigites is the following:

$$(100-n)\%\ \text{mass}\ (Bi_2Mo_3O_{12} + 0.6\ B_2O_3 + 0.7\ Na_2O) + n\%\ \text{mass}\left(\frac{(3-x)}{2}Mn_2O_3 + \frac{x}{2}Ni_2O_3 + 0.5\ B_2O_3\right) \quad (1)$$

Using this flux system, $Mn_{3-x}Ni_xBO_5$ compounds with x = 2.25, 2.17, and 0.5 were obtained.

In the concentration range of $0.5 \le x \le 2.25$ the crystallization of the black crystal phase was found to occur in the form of thin elongated prisms. This phase has the structure of natural ludwigite minerals. At $x < 0.5$, the crystallization of black flattened elongated prisms occurred, which was characterized as the phase of Mn_2BO_4 with the warwickite structure. In the range of about x = 2.25 there occurred the simultaneous crystallization of two phases: phase with the ludwigite type structure and the $Ni_3B_2O_6$ kotoite phase. Thus, the $Mn_{3-x}Ni_xBO_5$ ludwigite phase is a high-temperature one in a sufficiently wide range of nickel concentrations in the flux.

The concentration n in flux system (1) was chosen so that the corresponding saturation temperatures T_{sat} did not exceed the value T = 950 °C. Thus, the concentration range was $7\% \le n \le 15\%$. Due to the poor solubility of nickel oxide, the maximum value of concentration n = 15% corresponded to the composition with the minimum nickel content x = 0.5 (T_{sat} = 870 °C).

The saturation temperature T_{sat} was estimated by varying the temperature in the furnace and observing the crystal formation on the platinum rod used as a probe. The procedure includes several repeated steps of determining the T_{sat} range and its narrowing: 1 decreasing the temperature in the furnace to the temperature belonging to the range of the anticipated crystal and growth; 2 inserting the platinum probe to the flux after 20 s preheating near the flux surface; 3 removing the probe from the flux after 30 minutes, and depending on the presence or absence of the crystals on the rod the procedure is repeated (after homogenization) with a higher or lower temperature, respectively. T_{sat} is determined with an accuracy of about 2 °C.

Single crystals of $Mn_{3-x}Ni_xBO_5$ were grown using flux system (1) in accordance with the following temperature scenario. After homogenization of the flux at T = 1100 °C, the temperature in the furnace was reduced rapidly at a cooling rate of 100 °C h^{-1} down to (T_{sat} − 10)°C, and then slowly at a

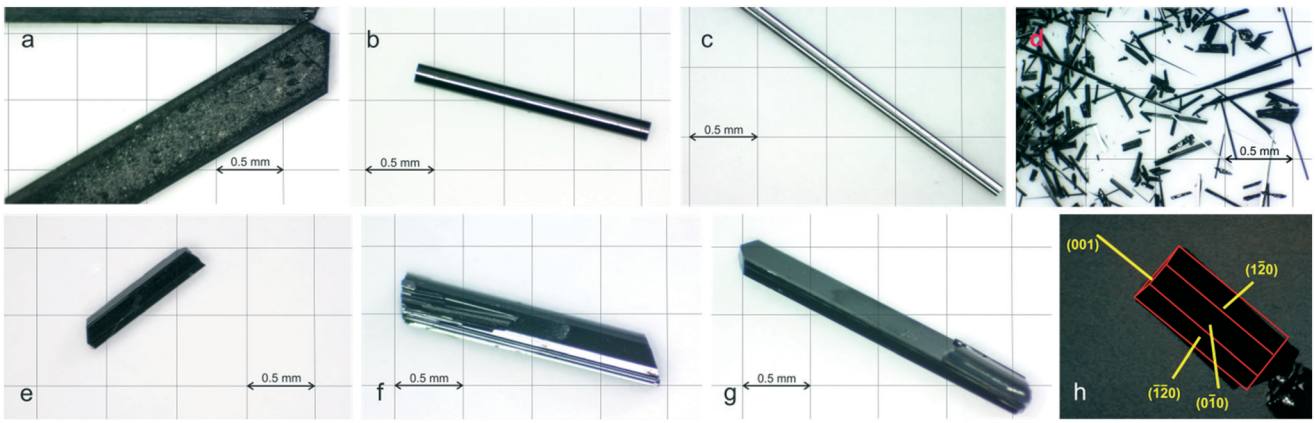

Fig. 2 Optical images of the obtained single crystals (the composition is given as in the flux): a – $Mn_{2.5}Ni_{0.5}BO_5$ (the white area is due to the facets with defects resulting from cleaning); b – $Mn_{1.5}Ni_{1.5}BO_5$; c – $MnNi_2BO_5$; d – $Mn_{0.75}Ni_{2.25}BO_5$; e – $MnNiCuBO_5$; f – $Mn_{0.75}Ni_{0.75}Cu_{1.5}BO_5$; g – $Mn_{1.97}Ni_{0.24}Cu_{0.79}BO_5$; h – the Miller indices for the facets of the obtained crystals. For the convenience and comparison, the images (a–g) are presented on the same scale.

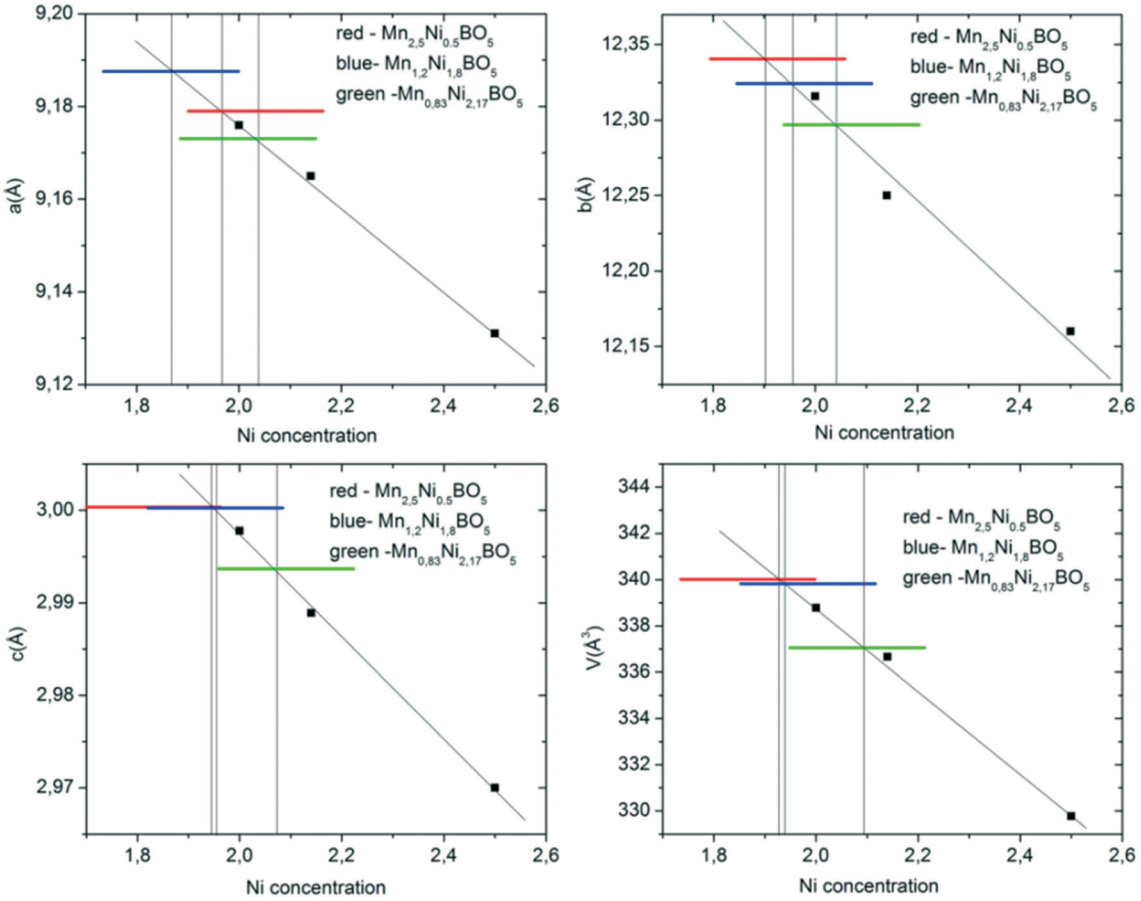

Fig. 3 Concentration dependences of the lattice parameters of $Mn_{3-x}Ni_xBO_5$ ludwigites. The values of the lattice parameters of $Mn_{3-x}Ni_xBO_5$ ludwigites with the unknown actual composition (only the ratio of the flux compounds) are denoted by horizontal color lines (red – $Mn_{2.5}Ni_{0.5}BO_5$, blue – $Mn_{1.2}Ni_{1.8}BO_5$, and green – $Mn_{0.83}Ni_{2.17}BO_5$). The vertical black lines indicate the crossing of the color lines and linear approximation trend of the benchmark compounds ($MnNi_2BO_5$, $Mn_{0.86}Ni_{2.14}BO_5$, $Mn_{0.5}Ni_{2.5}BO_5$), which is the actual composition of the studied ludwigites.

cooling rate of 4 °C per day. After three days, the crucible was removed from the furnace, and the flux was poured out. The single crystals grown were taken out of the crucible and etched in 20% aqueous solution of nitric acid to remove the remaining flux.

3.1.2 Li_2CO_3 – containing flux system. The initial Li-containing flux system for growing $Mn_{3-x}Ni_xBO_5$ ludwigites is the following:

$$(100-n)\%\ \text{mass}\ (Bi_2Mo_3O_{12} + 2.4\ B_2O_3 + 2\ Li_2O) + n\%\ \text{mass}\left(\frac{(3-x)}{2}Mn_2O_3 + \frac{x}{2}Ni_2O_3 + 0.5\ B_2O_3\right) \quad (2)$$

Using this flux system, $Mn_{3-x}Ni_xBO_5$ compounds with x = 1.5 and 1.8 were obtained. The preparation process of fluxes

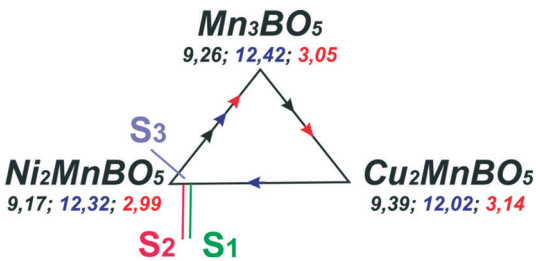

Fig. 4 Triple diagram of Mn_3BO_5–Ni_2MnBO_5–Cu_2MnBO_5 demonstrating the tendency of the lattice parameter change, depending on the cation composition of $(Mn,Ni,Cu)_3BO_5$ ludwigites. The green S1 (sample 1), pink S2 (sample 2) and lilac S3 (sample 3) points correspond to the Mn : Ni : Cu ratio in Tables 1 and 2.

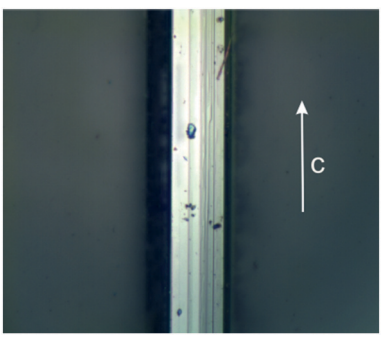

Fig. 5 Single crystal sample of $Mn_{1.5}Ni_{1.5}BO_5$ ludwigite chosen for the Raman experiment.

Table 1 Lattice parameters and ion coordinates of triple $(Mn,Ni,Cu)_3BO_5$ obtained by X-ray diffraction

		Sample 1 (1 : 1 : 1)			Sample 2 (1 : 1 : 2)			Sample 3 (2.5 : 0.3 : 1)		
Lattice parameters										
a, Å		9.1735(2)			9.1828(3)			9.19375(2)		
b, Å		12.2939(3)			12.2766(3)			12.33041(2)		
c, Å		3.00180(1)			3.0091(1)			3.016669(5)		
Ion coordinates										
		x/*a*	*y*/*b*	*z*/*c*	*x*/*a*	*y*/*b*	*z*/*c*	*x*/*a*	*y*/*b*	*z*/*c*
Me_1	2*a*	0	0	0	0	0	0	0	0	0
Me_2	2*d*	1/2	0	1/2	1/2	0	1/2	1/2	0	1/2
Me_3	4*g*	0.99797(2)	0.28037(2)	0	0.99851(4)	0.28029(4)	0	0.9972(5)	0.2807(2)	0
Me_4	4*h*	0.76006(3)	0.11554(2)	1/2	0.76055(5)	0.11582(4)	1/2	0.7613(4)	0.1165(3)	1/2
B	4*h*	0.7227(3)	0.36132(2)	1/2	0.7235(4)	0.3621(3)	1/2	0.712(3)	0.361(2)	1/2
O_1	4*g*	0.89374(2)	0.14346(1)	0	0.8939(3)	0.1436(2)	0	0.8935(10)	0.145(1)	0
O_2	4*h*	0.64702(2)	0.26408(1)	1/2	0.6476(3)	0.2642(2)	1/2	0.6525(11)	0.2612(9)	1/2
O_3	4*h*	0.85183(2)	−0.04187(1)	1/2	0.8517(3)	−0.0415(2)	1/2	0.8541(12)	−0.0416(9)	1/2
O_4	4*g*	0.61295(2)	0.08033(1)	0	0.6129(3)	0.0805(2)	0	0.6113(9)	0.0832(8)	0
O_5	4*h*	0.87372(2)	0.35900(1)	1/2	0.8738(3)	0.3596(2)	1/2	0.8724(1)	0.3568(1)	1/2

Table 2 Comparison of the lattice parameters and bond lengths of triple $(Mn,Ni,Cu)_3BO_5$ and Ni_2MnBO_5, Cu_2MnBO_5 ludwigites. Sample 1 – Mn : Ni : Cu = 1 : 1 : 1, sample 2 – Mn : Ni : Cu = 1 : 1 : 2, and sample 3 – Mn : Ni : Cu = 2.5 : 0.3 : 1

			Sample 1	Sample 2	Sample 3	Ni_2MnBO_5 (ref. 14 and 16)	Cu_2MnBO_5 (ref. 11)
	Pbam	$P2_1/c$	*Pbam*	*Pbam*	*Pbam*	*Pbam*	$P2_1/c$
Bonds	Number of bonds		*d*, Å				
Mn : Ni : Cu			1 : 1 : 1	1 : 1 : 2	2.75 : 0.3 : 1		
Me_1–O	2	2	2.0151(1)	2.0142(2)	2.033	2.02	1.95
Me_1–O	4	2	2.0893(1)	2.0923(2)	2.082	2.08	1.99
		2		—		—	2.44
Me_2–O	2	2	2.0740(1)	2.0770(3)	2.120	2.09	1.91
Me_2–O	4	2	2.0849(1)	2.0773(2)	2.091	2.07	1.96
		2		—		—	2.61
Me_3–O	1	1	1.9358(1)	1.9336(3)	1.931	1.94	1.90
Me_3–O	1	1	2.0114(2)	2.0060(3)	1.977	2.026	1.94
Me_3–O	2	2	2.1026(1)	2.1063(2)	2.115	2.09	2.02
Me_3–O	2	1	2.1181(1)	2.1268(2)	2.140	2.11	2.39
		1		—		—	2.50
Me_4–O	2		1.9683(1)	1.9696(2)	1.967	1.96	1.90
Me_4–O	2		2.0643(1)	2.0712(2)	2.085	2.06	2.00
Me_4–O	1		2.1000(1)	2.0962(3)	2.046	2.105	2.20
Me_4–O	1		2.1103(1)	2.1049(3)	2.013	2.111	2.38
Cell parameters							
a, Å			9.1735(2)	9.1828(3)	9.19375(2)	9.176(1)	9.3973(2)
b, Å			12.2939(3)	12.2766(3)	12.33041(2)	12.316(2)	12.0242(3)
c, Å			3.00180(1)	3.0091(1)	3.016669(5)	2.9978(4)	3.14003(7)

(2) is analogous to the previously described one for the Na-containing system (1). The only difference is the replacement of Na_2CO_3 carbonate with Li_2CO_3 and a significant increase of the boron oxide weight coefficient. As in the case of Na_2CO_3, Li_2CO_3 decomposes under heating with the release of CO_2: $Li_2CO_3 \rightarrow Li_2O + CO_2\uparrow$.

The concentration *n* of the crystal-forming oxides in these fluxes are $n_1(x = 1.5) = 11\%$ and $n_2(x = 1.8) = 8\%$. The corresponding saturation temperatures are $T_{sat1} = 935$ °C and $T_{sat2} = 900$ °C.

The high-temperature crystallizing phase of flux system (2) in a wide temperature range (not lower than 50 °C) is the phase of black elongated prisms, *i.e.* ludwigite phase which was determined by powder X-ray analysis. The growth procedure for these compositions is analogous to the previously mentioned one for system (1).

3.2 Flux growth of triple $(Mn,Ni,Cu)_3BO_5$ ludwigites

To study the competition between Cu^{2+} and Ni^{2+} bivalent cations during the crystal formation of ludwigites and to obtain new compounds with perspective properties, triple $(Mn,Ni,Cu)_3BO_5$ ludwigites were grown with different ratios of Mn/Ni/Cu. Three compositions were obtained:

1. Mn : Ni : Cu = 1 : 1 : 1;
2. Mn : Ni : Cu = 1 : 1 : 2;

3. Mn : Ni : Cu = 2.75 : 0.3 : 1.

Compositions **1** and **2** were obtained by the addition of CuO to flux system (2) with the ratio Mn/Ni = 1. The ratio of the components of the corresponding fluxes can conveniently be written as:

(1) $Bi_2Mo_3O_{12}$: 2.57 B_2O_3 : 2 Li_2O : 0.33 Mn_2O_3 : 0.33 Ni_2O_3 : 0.66 CuO

(2) $Bi_2Mo_3O_{12}$: 2.57 B_2O_3 : 2 Li_2O : 0.33 Mn_2O_3 : 0.33 Ni_2O_3 : 1.32 CuO

After adding CuO, the analysis of the flux parameters shows small changes: T_{sat} of (1) did not change, corresponding to T_{sat} = 935 °C for $Mn_{1.5}Ni_{1.5}BO_5$, while T_{sat} of (2) increased by 5 °C and was equal to $T_{sat(2)}$ = 940 °C. The high-temperature phase did not change, this being the phase with the ludwigite type structure. At the crystal growth stage the fluxes were homogenized at T = 1100 °C. The growth procedure is analogous to that used for growing double Mn–Ni ludwigites: after homogenization the temperature in the furnace was reduced rapidly at a cooling rate of 100 °C h^{-1} down to (T_{sat} − 10) °C, and then, slowly at a cooling rate of 4 °C per day. After three days, the crucible was removed from the furnace, and the flux was poured out. The grown crystals had the same shape as double $(Mn,Ni)_3BO_5$ ludwigites. Except for $Mn_{2.5}Ni_{0.5}BO_5$ (with a high Mn_2O_3 concentration in the flux) which had the shape of flattened prisms. However, the size of the grown single crystals increased by about 3 times, amounting to 0.3 × 0.3 × 4 mm^3. The images of the triple $(Mn,Ni,Cu)_3BO_5$ and double $(Mn,Ni)_3BO_5$ ludwigites with the size denoted are presented in Fig. 2, including the Miller indices for the facets of the obtained crystals.

Composition **3** was obtained by the addition of Ni_2O_3 to the flux system for growing $(Mn,Cu)_3BO_5$ oxyborates:

$$75\%\ \text{mass}\ (Bi_2Mo_3O_{12} + 0.9\ B_2O_3 + 1.4\ Na_2O) + 25\%\ \text{mass}\ (1.1\ Mn_2O_3 + 0.8\ CuO + 0.5\ B_2O_3) \quad (3)$$

The weight coefficient of Na_2O increased proportionally to the weight of Mn_2O_3 oxide to fix the 3+ valence state of the manganese cations.[25] After adding Ni_2O_3, the ratio of the components in this flux system can be written as: $Bi_2Mo_3O_{12}$: 2.48 B_2O_3 : 1.4 Na_2O : 1.35 Mn_2O_3 : 0.98 CuO : 0.16 Ni_2O_3. Before adding Ni_2O_3, the high-temperature phase in this system was the phase of black flattened elongated prisms, which was characterized as $Mn_{2-x}Cu_xBO_4$, with the corresponding saturation temperature being T_{sat} = 835 °C. The addition of Ni_2O_3 (m = 1.5 g, m_{flux} = 83.8 g) led to an increase in the saturation temperature up to T_{sat} = 980 °C. Thus, adding m = 1 g of Ni_2O_3 increased the saturation temperature up to ≈ 100 °C. As a result of adding nickel oxide, there occurred the transformation of the high-temperature phase to the ludwigite phase. The crystal growth procedure is the same as that being used for other compositions, the growth time was 3 days, and the growth cooling rate was 4 °C per day. The habit of the grown crystals of **3** slightly differs from $(Mn,Ni)_3BO_5$ and $(Mn,Ni,Cu)_3BO_5$ ludwigites: the $(1\bar{2}0)$ facets are poorly pronounced (Fig. 2). The change in the shape may be accounted for the large amount of Mn_2O_3 in the flux and, possibly, larger copper concentration in the crystal. As in the case of $(Mn,Ni,Cu)_3BO_5$ with compositions **1** and **2**, the size of the obtained crystals is suitable for the study of orientational dependences of physical properties (*e.g.* magnetization).

4. Crystal structure

Ludwigites belong to the *Pbam* (No. 55) space group. In the ludwigite structure, metallic cations occupy 4 positions: 4*g*, 4*h*, 2*a*, and 2*d*. The 4*h* position is more often occupied by trivalent (or tetravalent) ions which are also partly located in the 2*d* position. The 2*a* and 4*g* positions are predominantly occupied by bivalent ions.[26]

The structure and phase homogeneity of the synthesized crystals were analyzed by powder X-ray diffraction. The XRD analysis revealed no additional peaks, indicating the phase purity for each individual sample. The phase, space group and lattice parameters were determined and controlled during the growth stage.

4.1 Actual composition of double $(Mn,Ni)_3BO_5$ ludwigites using powder X-ray diffraction

The Ni concentration dependences of the lattice parameters and unit cell volume, obtained by powder X-ray diffraction, are presented in Fig. 2, including the data for $Mn_{0.5}Ni_{2.5}BO_5$ provided in the literature.[27] As it was mentioned in the crystal growth section, $(Mn,Ni)_3BO_5$ ludwigites exist in a wide range of nickel concentrations in the flux. The actual cation composition and valence states of the metal ions of $Mn_{3-x}Ni_xBO_5$ ludwigites for x = 1.5 and 2.25 were refined earlier by the EXAFS and XANES element-selective techniques.[14,15] The actual composition of the studied $(Mn,Ni)_3BO_5$ ludwigites was analyzed using these compounds as a benchmark. In the benchmark compounds, manganese ions are predominantly in the trivalent state. As a result of refinement, the actual composition of $Mn_{1.5}Ni_{1.5}BO_5$ (in the flux) is $MnNi_2BO_5$,[14] and the actual composition of $Mn_{0.75}Ni_{2.25}BO_5$ (in the flux) is $Mn_{0.86}Ni_{2.14}BO_5$.[15] In $Mn_{0.86}Ni_{2.14}BO_5$, manganese ions are both in trivalent and tetravalent states. As can be seen, the dependences are linear and in good agreement with Vegard's law. Using Vegard's law, the actual composition of the other $Mn_{3-x}Ni_xBO_5$ compounds was estimated. In Fig. 3 these values are denoted by the crossing of color lines (the experimental values of the lattice parameters and unit cell volumes) and vertical black lines. It is clearly seen that the actual compositions are close to $MnNi_2BO_5$ despite quite a wide variation of nickel concentrations in the flux.

4.2 Analysis of the structural parameters of $(Mn,Ni,Cu)_3BO_5$ ludwigites

The crystal structure of triple ludwigites was refined using powder and single crystal X-ray diffraction. Sample 1 with

Mn : Ni : Cu = 1 : 1 : 1 and sample 2 with Mn : Ni : Cu = 1 : 1 : 2 were investigated by single crystal XRD, while the structural parameters of sample 3 with Mn : Ni : Cu = 2.5 : 0.3 : 1 was investigated by powder XRD. The results of the refinement are presented in Tables 1 and 2. In these tables, metallic ions (Cu, Mn, Ni) are denoted as "Me" because it is extremely difficult to clarify the concentrations of Cu, Ni and Mn ions in different positions using the X-ray diffraction method. As shown in Tables 1 and 2, the crystal structure of all three compounds $(Ni,Cu,Mn)_3BO_5$ belongs to the *Pbam* space group. The crystal cell of the studied samples is orthorhombic. This indicates that monoclinic distortion due to the Jahn–Teller effect of Cu ions does not appear, and the concentration of Cu ions in the compounds is not high.

The structural data of the parent compounds (Ni_2MnBO_5 and Cu_2MnBO_5) and studied samples were compared and some assumptions were made about the distribution of metallic ions over the positions. For sample 1 and sample 2 (see Table 1), the lattice parameters are similar to those for Ni_2MnBO_5. The distances of Me–O for all the oxygen octahedra are also similar to those for Ni_2MnBO_5. We suggest that in samples 1 and 2, Mn ions should be predominantly trivalent as in Ni_2MnBO_5 (as confirmed by EXAFS and XANES[14]). The positions Me1–Me3 are occupied by Ni and Cu ions, Me4 being occupied by Mn ions. In this case, the chemical formula for the studied compounds will be $Ni_{2-x}Cu_xMnBO_5$. Assuming Vegard's law for the lattice parameters to be true for $Ni_{2-x}Cu_xMnBO_5$ as well, the concentrations of Cu ions are estimated, which are lower than 10 percent for all the compounds (Fig. 3).

In sample 3 the content of Mn in the flux significantly exceeds the content of other metals. The structural parameters of sample 3 differ from those of samples 1 and 2. Fig. 4 shows the lattice parameters for the three compounds: Ni_2MnBO_5, Mn_3BO_5 and Cu_2MnBO_5. The *a* and *c* parameters increase from Ni_2MnBO_5 to Mn_3BO_5, and Cu_2MnBO_5 (the black and red arrows). The *b* lattice parameter increases from Cu_2MnBO_5 to Ni_2MnBO_5 and Mn_3BO_5 (the blue arrows). As one can see in Table 1, the *b* lattice parameter for sample 3 is greater than that for Cu_2MnBO_5 and Ni_2MnBO_5. It is suggested that in sample 3, Mn ions are in bivalent and trivalent states as in Mn_3BO_5. This assumption is in agreement with the high Mn_2O_3 concentration in the flux. These differences in structure are consistent with the changes in the habit of this sample as compared to other $(Mn,Ni,Cu)_3BO_5$ ludwigites.

4.3 Analysis of the crystal composition and homogeneity

The six groups of samples with different compositions were molded into plastic and then mechanically polished (Fig. S1†). The EDX spectra analysis showed that the samples were homogeneous in composition both inside and across the needles. In order to test the homogeneity, we compared the spectra of different sections of the crystals for all the six groups of the samples. In Fig. S2,† the images of the crystals from each of the six groups are shown. The images present sections which were chosen to compare the spectra. In Fig. S3,† the spectra for each section of the crystal were presented. As one can see in Fig. S3,† the spectra are almost identical, indicating the homogeneity of the samples. The ratios of Mn : Ni : Cu in the flux and in the crystal are presented in Table 3. As one can see in Table 3, the ratio of Mn : Ni : Cu in the crystal is significantly different from that in the flux. In all the crystals the nickel content is higher than that of copper. Despite the higher content of copper in the flux, its quantity is much smaller in the crystal.

5. Polarized Raman spectra

Polarized Raman spectra were obtained at room temperature for the two samples with the addition of copper and without it: the ratios Mn : Ni = 1 : 1 and Mn : Ni : Cu = 1 : 1 : 1 were taken as it was done in the flux.

Two series of experiments were conducted with the parallel (HH) and cross-parallel (HV) polarization of incident and scattered beams to study the angular dependence of the intensities of the Raman spectral lines on the polarization direction of the incident and scattered radiation. The backscattering geometry was used. The shift of the incidence point of exciting radiation was smaller than 2 μm in complete revolution by 2π. The angular step was 10°. The Raman intensity maps, depending on the rotation angle of the studied samples in the spectral range of 20 ÷ 1100 cm^{-1}, are shown in Fig. 6. These maps were obtained for HH and HV polarizer configurations. The HH polarization mode corresponds to the rotation of the polarization vector in the needle plane (the view plane in Fig. 5). The HV polarization mode corresponds to the rotation of the polarization vector in the plane perpendicular to the *c* axis. The spectra of both compounds are very similar to each other. Conditionally, the spectra could be divided into some spectral ranges. The low spectral range up to 200 cm^{-1} contains lines of lattice vibrations; 200 ÷ 600 cm^{-1} contains MeO_6 octahedra vibration modes; and the spectral range of >600 cm^{-1} includes vibrations of the BO_3 groups.[28]

Based on the Raman maps, the data of the studied samples were compared at different rotation angles in the spectral range of 20 ÷ 1500 cm^{-1}; for the HV configuration, the angles were taken to be 0° and 45°, while for the HH configurations, they were taken to be 0° and 90°. The results

Table 3 Comparison of the Mn : Ni : Cu ratio in the flux and those obtained by EDX

Sample No.	Double or triple ludwigite	Mn : Ni : Cu ratio in the flux	Mn : Ni : Cu ratio in the crystal
1	$(Mn,Ni)_3BO_5$	1 : 1 : 0	1 : 2.36 : 0
2		1 : 1.5 : 0	1 : 2.5 : 0
3		5 : 1 : 0	1 : 1.76 : 0
4	$(Mn,Ni,Cu)_3BO_5$	1 : 1 : 1	1 : 1.89 : 0.15
5		1 : 1 : 2	1 : 1.9 : 0.3
6		2.5 : 0.3 : 1	1 : 1.42 : 0.26

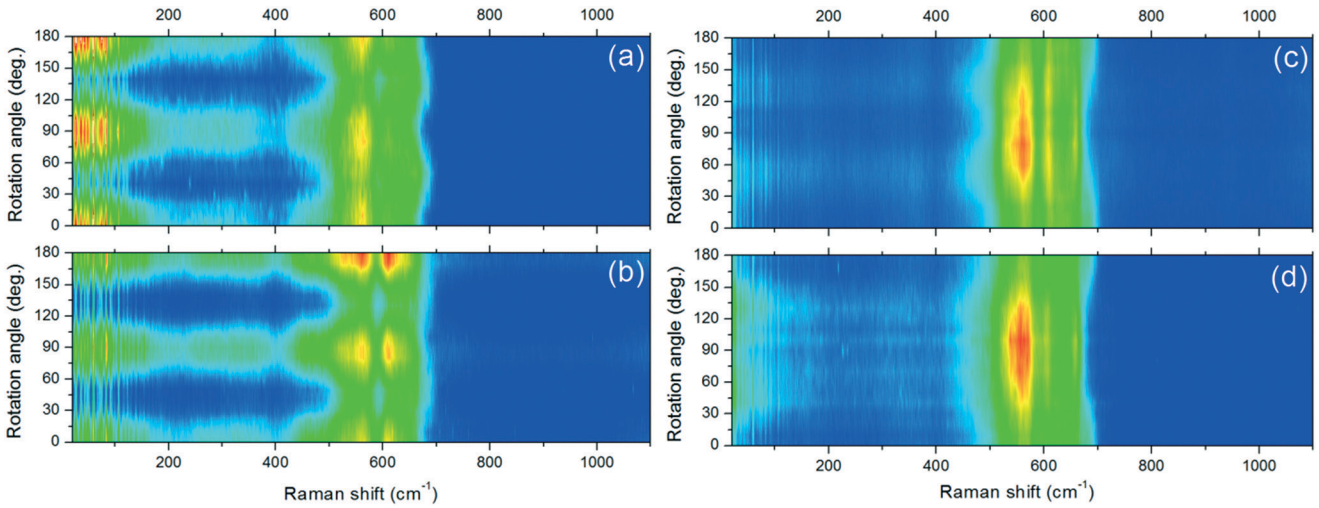

Fig. 6 Intensity maps of $(Mn,Ni)_3BO_5$ (Mn : Ni = 1 : 1) and $(Mn,Ni,Cu)_3BO_5$ (Mn : Ni : Cu = 1 : 1 : 1) ludwigites, depending on the rotation angle: a – HV mode of $(Mn,Ni,Cu)_3BO_5$ (Mn : Ni : Cu = 1 : 1 : 1); b – HV mode of $(Mn,Ni)_3BO_5$ (Mn : Ni = 1 : 1); c – HH mode of $(Mn,Ni,Cu)_3BO_5$ (Mn : Ni : Cu = 1 : 1 : 1); d – HH mode of $(Mn,Ni)_3BO_5$ (Mn : Ni = 1 : 1).

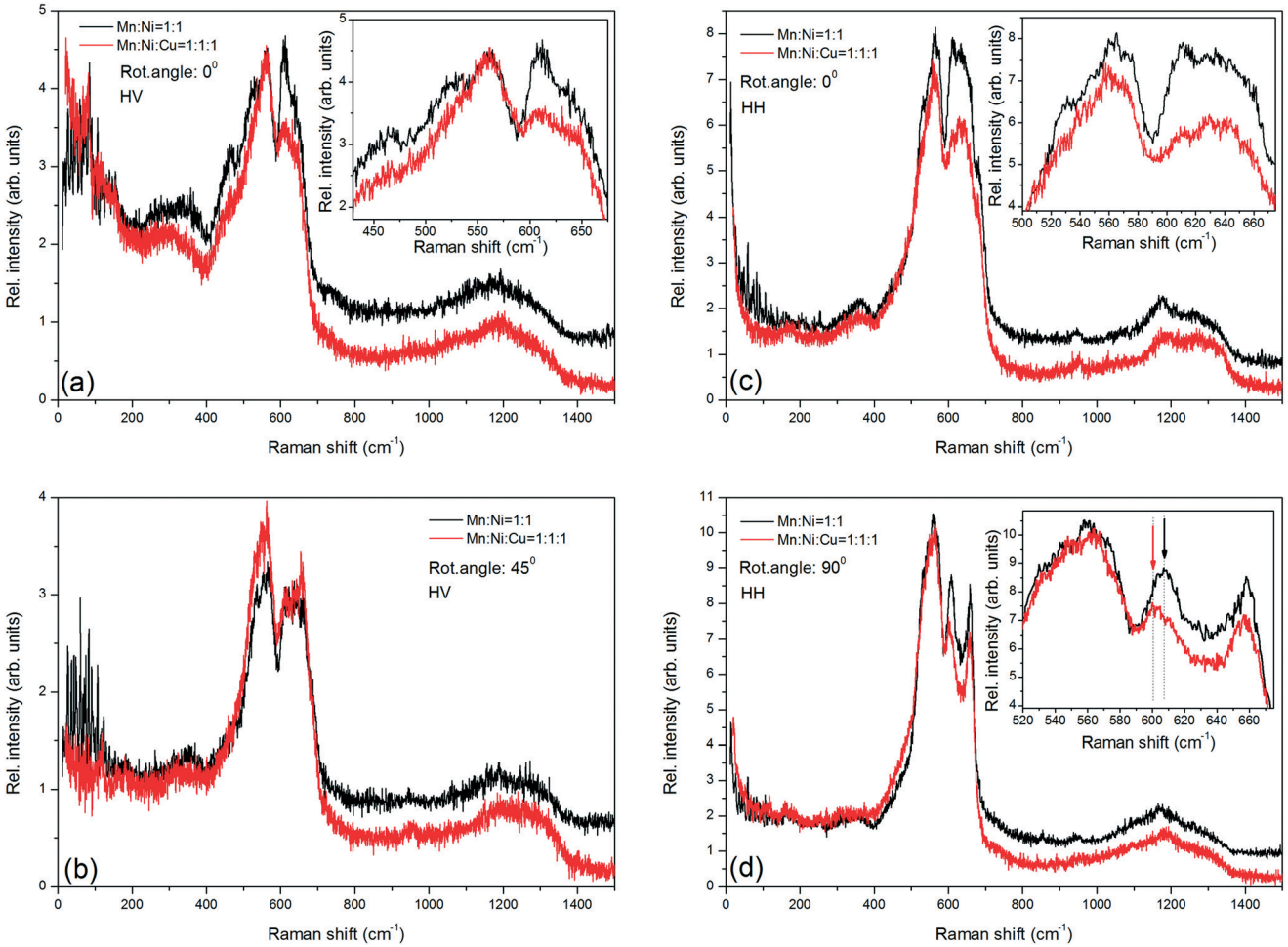

Fig. 7 Comparison of the Raman spectra of $(Mn,Ni)_3BO_5$ (Mn : Ni = 1 : 1) and $(Mn,Ni,Cu)_3BO_5$ (Mn : Ni : Cu = 1 : 1 : 1) ludwigites at different values of the rotation angle in two HH and HV polarization modes: a – 0°, HV mode; b – 45°, HV mode; c – 0°, HH mode; d – 90°, HH mode.

are shown in Fig. 7. As one can see, the most significant changes could be observed in the most intensive band within the range of 400 ÷ 700 cm^{-1}. The main changes of the spectra are the different ratios of the intensities. Here, the intensities of some spectra within the spectral range of 450 ÷ 580 cm^{-1} show substantial differences only at the rotation angle = 0° in the HV mode, without any shift in the line centers. Here, the spectral range of 580 ÷ 670 cm^{-1} shows a number of pronounced changes upon adding copper: the intensity of this spectral part is much lower than it was previously described. However, at a rotation angle of 90° in the HH polarization configuration there is a shift in the position of the line center as indicated by the arrows in the inset of Fig. 7d.

Analyzing the polarized Raman spectra changes of the two Mn/Ni and Mn/Ni/Cu ludwigite samples with and without copper, respectively, one can see that despite the similarity, there are minor differences in the spectral part containing the MeO_6 octahedral vibrational modes. These differences could indicate the crystal structure changes arising due to the presence of copper.

6. Discussion

The possibility of obtaining single crystals of heterovalent $(Mn,Ni)_3BO_5$ and $(Mn,Ni,Cu)_3BO_5$ ludwigites by the flux method is shown. The crystallization of these compounds is studied in complex flux systems based on $Bi_2Mo_3O_{12}$–B_2O_3 diluted with sodium or lithium carbonates. This solvent (with Na_2CO_3) was used earlier for growing other ludwigites[25] and it is characterized by a low viscosity and a wide working temperature range. As shown in ref. 25, different components of the solvent play an important role in the crystallization of Mn-heterovalent compounds. The absence of the Mn^{3+}-containing phase in the flux system $Bi_2Mo_3O_{12}$–B_2O_3–Mn_2O_3 without adding Na_2CO_3 was experimentally established.

Li and Na carbonates play an important role in the Mn^{3+} valence state stabilization. The influence of Na_2CO_3 on the Mn^{3+}-containing phase crystallization in the $Bi_2Mo_3O_{12}$–Na_2CO_3–B_2O_3 fluxes is described in detail in ref. 20. The approach presented in ref. 20 suggests the formation of intermediate chemical bonds in the flux – $Mn^{2+}MoO_4$ and $Mn^{3+}NaO_2$, which can fix the Mn^{2+} and Mn^{3+} valence states. The existence of the $Mn^{2+}MoO_4$ phase in the above mentioned fluxes was experimentally proved and it was observed as a high-temperature crystallizing phase. The existence of the Mn^{3+}-NaO_2 intermediate bonds was not experimentally confirmed. However, the addition of Na_2CO_3 results in the crystallization of the Mn^{3+}-containing phases (Mn_3O_4 and Mn_2O_3 oxides, Mn-containing warwickites and ludwigites), while in the absence of Na_2CO_3 it is possible to obtain only $Mn^{2+}MoO_4$.

Delafossite structured $A^{3+}B^{1+}O_2$ compounds are rather numerous and include $Mn^{3+}NaO_2$,[29] $Mn^{3+}LiO_2$,[30] $Ni^{3+}NaO_2$,[31] and $Ni^{3+}LiO_2$ (ref. 32) despite a large difference in Li^{1+} and Na^{1+} ionic radii. Thus, the existence of all these compounds suggests a possibility of $Mn^{3+} \rightarrow Ni^{3+}$ substitutions in the trivalent subsystem in the presence of lithium or sodium carbonates. However, the investigation of the valence composition of two $(Mn,Ni)_3BO_5$ ludwigites[14,15] by high precision element selective techniques (EXAFS and XANES) showed no Ni^{3+} cations in these materials. Even in the case of $Ni_{2.25}Mn_{0.75}BO_5$ with $x > 2$ the Mn^{4+} presence is more energy favorable for compensating the charge than the Ni^{3+} cation formation in the crystal.

The addition of Li_2CO_3 or Na_2CO_3 does not promote the appearance of Ni^{3+} cations in the ludwigite crystal, but can stabilize the 3+ manganese valence state. This was confirmed by the presence of the ludwigite phase in the Li_2CO_3-diluted fluxes (2). Besides, using Li_2CO_3 expands the growth capabilities of the studied fluxes due to the other eutectic positions on the Li_2O–B_2O_3 phase diagram.[19] The eutectic point of the Li_2O–B_2O_3 phase diagram is located at about 19 wt% of Li_2O, while in the Na_2O–B_2O_3 phase diagram it is located at about 70–75 wt% of Na_2O (using a lower percentage of oxide drastically increases the melting temperature of the mixture). This explains the significant differences in the weight ratio of boron and alkaline metal oxides. B_2O_3 oxide has the lowest melting temperature as compared to the components of the flux. It provides the middle saturation temperatures and allows one to avoid the high temperature range where significant evaporation of the flux (in particular, MoO_3) is observed. But an essential disadvantage of using B_2O_3 as a solvent is high viscosity. $Bi_2Mo_3O_{12}$–B_2O_3–Na_2CO_3 (Li_2CO_3) has low viscosity due to bismuth trimolybdate which compensates the B_2O_3 contribution. Thus, the weight coefficients of (1–3) were experimentally determined based on the flux viscosity, working temperatures, and $B_2O_3/Na_2O(Li_2O)$ ratio, taking into account their binary phase diagrams.

Unlike $Mn_{3-x}Cu_xBO_5$ with quite a narrow concentration range of the ludwigite phases ($1.2 \leq x \leq 0.75$), $Mn_{3-x}Ni_xBO_5$ ludwigites are characterized by quite a wide concentration range $2.5 \leq x \leq 0.75$ (x corresponds to the Ni content in the flux). However, the structural characterization by X-ray diffraction shows the inconsistency between the concentration x in the crystal and the concentration in the flux. The nickel concentration x in all the five $(Mn,Ni)_3BO_5$ compounds obtained is about 2. This is especially pronounced for the compositions with x = 0.5, 1.5, and 1.8. However, the concentration of the compounds with x = 2.13 and x = 2.25 in the flux is very close to the actual one, and these compounds are characterized by the presence of manganese ions with the 4+ valence state. The inconsistency of the nickel concentration in the crystals and its concentration in the flux can be related to the poor solubility of nickel oxide in the fluxes used, especially in comparison with the solubility of manganese oxide. Consequently, the ratio between the solubility coefficients of nickel and manganese is such that nickel enters the crystal predominantly and almost fully occupies the divalent subsystem. Manganese ions enter the crystal as a residue and finish building the trivalent subsystem.

As concerns multicomponent fluxes, the phase formation can in some cases be hardly controlled and predicted. This is due to the competition of chemical bonds of many different components of the flux. It is necessary to specify the role of each flux component in the formation of the desirable crystal phase and possible secondary phases. This study deals with the complex solvent and complex soluble substance. It is a well-known fact that the real composition of the growing crystals can significantly be different from the concentration of the crystal forming initial components in the flux.

In the case of the studied double $(Mn,Ni)_3BO_5$ and triple $(Mn,Ni,Cu)_3BO_5$ ludwigites in the flux there are three/four cation types: Mn^{3+}, Mn^{2+}, and Ni^{2+} (Cu^{2+}). The unit cell contains 4 non-equivalent cation positions which can be occupied by these cations with different probabilities, with the conservation of electroneutrality. Therefore, the distribution of the cations depends both on crystal-chemical factors, such as special octahedral symmetry formed due to the Jahn–Teller effect of Cu^{2+} and its selectivity due to that, and the flux chemistry, including the solubility of the initial components and, as a consequence, the distribution coefficients of different cations. As ludwigites are heterovalent and for many discussed compounds there is (2+, 3+) combination of heterovalent cations, where the 3+ cation is only Mn^{3+}. The bivalent subsystem can be represented by Mn^{2+}, Ni^{2+} and Cu^{2+} in the case of triple ludwigites. Thus, there is some competition between these cations in the flux at the stage of the crystal formation which gives rise to the real composition of the synthesized materials. The study of this competition and understanding of its origin and peculiarities will allow obtaining compounds with the desired composition, to enhance the flux crystallization control.

It was experimentally shown that there was a small amount of copper in the grown crystals in almost all the studied compounds, even in the sample with ratio Mn : Ni : Cu = 1 : 1 : 2 in the flux, with the weight of copper exceeding that of nickel by two times. One can make a conclusion concerning a strong dependence of the crystal composition of $(Mn,Ni,Cu)_3BO_5$ ludwigites on a huge difference in the solubility of the CuO and NiO (Ni_2O_3) oxides. Thus, the distribution coefficient of NiO (Ni_2O_3) is such that almost the entire bivalent subsystem is represented by Ni^{2+} cations. The partial saturation of the flux by NiO (Ni_2O_3) is higher and this component is first removed from the flux. In order to obtain a high-copper containing triple $(Mn,Ni,Cu)_3BO_5$ ludwigite it is necessary to increase the CuO concentration by several times. This will enhance the partial copper saturation in the flux and let Cu^{2+}, along with Ni^{2+}, enter the crystal.

The addition of copper to $Mn_{3-x}Ni_xBO_5$ ludwigites leads to no explicit changes in the structure regardless of the amount of the additive, as evidenced by X-ray diffraction analysis. There are small changes in the lattice parameters and bond lengths in agreement with the increase in the Cu/Ni ratio (Tables 1 and 2). These changes are not accompanied by the change of the space group into monoclinic $P2_1/c$ which is characteristic of Mn–Cu ludwigites. All the obtained Mn/Ni/Cu ludwigites have the symmetry of $(Mn,Ni)_3BO_5$, and they are orthorhombic with the space group *Pbam*. The lattice parameters and bond lengths of Mn/Ni/Cu ludwigites are closer to those of Ni_2MnBO_5 than to the same values of Cu_2MnBO_5 (see Table 2).

The polarized Raman spectra of the single crystals with the ratios in the flux Mn : Ni = 1 : 1 and Mn : Ni : Cu = 1 : 1 : 1 also show some changes in the spectra after adding copper: different intensity ratios and shifting of the center position in the spectral range of 600 ÷ 620 cm^{-1} in the HH mode, rot. angle = 90°. The character of these changes also indicates that copper is present in the structure of $Mn_{3-x}Ni_xBO_5$:Cu, but its concentration is much lower than the concentration in the flux. The phenomenon of low copper concentration in $(Mn,Ni,Cu)_3BO_5$ ludwigites can also be explained by a great difference in the solubility of nickel and copper. In this case, copper may be considered as a solvent component. Despite small changes in the composition, the addition of copper noticeably influences the size of the single crystal, which is increased by up to 3 times.

7. Conclusions

This study presents a method of the flux growth of several compounds of double $(Mn,Ni)_3BO_5$ and triple $(Mn,Ni,Cu)_3BO_5$ ludwigites. The suggested flux systems are well worked out, comprising compounds capable of influencing the crystallization of Mn^{2+} and Mn^{3+} containing phases, allowing one to control this part of the crystallization process. The structure and actual composition of the grown single crystals were studied by X-ray diffraction. A conclusion is made that the nickel concentration in all the five compounds obtained is quite different from the concentration in the flux and it is close to 2. Along with the X-ray diffraction of $(Mn,Ni)_3BO_5$ and $(Mn,Ni,Cu)_3BO_5$ compounds, the polarized Raman spectra of the compounds with the ratios in the flux Mn : Ni = 1 : 1 and Mn : Ni : Cu = 1 : 1 : 1 were analyzed which shows copper entering the $Mn_{3-x}Ni_xBO_5$: Cu crystals but with a small copper concentration.

Since we were able to obtain the single crystals of sufficient size, the next stage of studying $(Mn,Ni)_3BO_5$ and $(Mn,Ni,Cu)_3BO_5$ is to investigate complex properties using element-selective EXAFS and XANES techniques, orientational magnetometry, specific heat and MCE. It is necessary to continue growth experiments with an increased amount of copper. Thus it will be possible to achieve a comparable Ni/Cu ratio in the crystal and to determine the orthorhombic–monoclinic phase boundary for $(Mn,Ni,Cu)_3BO_5$ ludwigites.

Author contributions

Evgeniya Moshkina: conceptualization, methodology, investigation, writing – original draft Asya Bovina: investigation, resources Maxim Molokeev: investigation, resources Alexander Krylov: investigation, resources

Alexander Shabanov: investigation, resources Artem Chernyshov: investigation, resources Svetlana Sofronova: supervision, writing – review & editing, data curation.

Conflicts of interest

There are no conflicts to declare.

Acknowledgements

This work was supported by the Russian Foundation for Basic Research, the Government of the Krasnoyarsk Krai, and the Krasnoyarsk Territorial Foundation for Support of Scientific and R&D Activities, project no. 20-42-240011. X-ray and EDX data were obtained with the use of the analytical equipment of the Krasnoyarsk Regional Center of Research Equipment of Federal Research Center "Krasnoyarsk Science Center SB RAS".

References

1 S. R. Bland, M. Angst, S. Adiga, V. Scagnoli, R. D. Johnson, J. Herrero-Martín and P. D. Hatton, Symmetry and charge order in Fe_2OBO_3 studied through polarized resonant x-ray diffraction, *Phys. Rev. B: Condens. Matter Mater. Phys.*, 2010, **82**, 115110.

2 N. B. Ivanova, N. V. Kazak, V. Knyazev Yu, D. A. Velikanov, A. D. Vasiliev, L. N. Bezmaternykh and M. S. Platunov, Structure and magnetism of copper-substituted cobalt ludwigite $Co_3O_2BO_3$, *Low Temp. Phys.*, 2013, **39**(8), 709–713.

3 C. W. Galdino, D. C. Freitas, C. P. C. Medrano, R. Tartaglia, D. Rigitano, J. F. Oliveira, A. A. Mendonça, L. Ghivelder, M. A. Continentino, D. R. Sanchez and E. Granado, Magnetic, electronic, structural, and thermal properties of the $Co_3O_2BO_3$ ludwigite in the paramagnetic state, *Phys. Rev. B*, 2019, **100**, 165138.

4 F. Damay, J. Sottmann, F. Lainé, L. Chaix, M. Poienar, P. Beran, E. Elkaim, F. Fauth, L. Nataf, A. Guesdon, A. Maignan and C. Martin, Magnetic phase diagram for $Fe_{3-x}Mn_xBO_5$, *Phys. Rev. B*, 2020, **101**, 094418.

5 E. M. Moshkina, T. P. Gavrilova, I. F. Gilmutdinov, A. G. Kiiamov and R. M. Eremina, Flux crystal growth of Cu_2GaBO_5 and Cu_2AlBO_5, *J. Cryst. Growth*, 2020, **545**, 125723.

6 J. Kumar, S. N. Panja, D. J. Mukkattukavil, A. Bhattacharyya, A. K. Nigam and S. Nair, Reentrant super spin glass state and magnetization steps in the oxyborate Co_2AlBO_5, *Phys. Rev. B*, 2017, **95**, 144409.

7 J. Schaefer and K. Bluhm, Zur Kristallstruktur von Cu2M(BO3)O2 (M=Fe3+, Ga3+), *Z. Anorg. Allg. Chem.*, 1995, **621**, 571–575.

8 A. Utzolino and K. Bluhm, Synthesis and X-Ray Characterization of Two New Compounds with Ludwigite-Structure: $Co_5Sn(BO_3)_2O_4$ and $Co_5Mn(BO_3)_2O_4$, *Z. Naturforsch., A: Phys. Sci.*, 1996, **51b**, 305–308.

9 M. A. V. Heringer, D. L. Mariano, D. C. Freitas, E. Baggio-Saitovitch, M. A. Continentino and D. R. Sanchez, Spin-glass behavior in $Co_3Mn_3(O_2BO_3)_2$ ludwigite with weak disorder, *Phys. Rev. Mater.*, 2020, **4**, 064412.

10 E. Moshkina, C. Ritter, E. Eremin, S. Sofronova, A. Kartashev, A. Dubrovskiy and L. Bezmaternykh, Magnetic structure of Cu_2MnBO_5 ludwigite: thermodynamic, magnetic properties and neutron diffraction study, *J. Phys.: Condens. Matter*, 2017, **29**, 245801.

11 S. Sofronova, E. Moshkina, I. Nazarenko, Yu. Seryotkin, S. A. Nepijko, V. Ksenofontov, K. Medjanik, A. Veligzhanin and L. Bezmaternykh, Crystal growth, structure, magnetic properties and theoretical exchange interaction calculations of Cu_2MnBO_5, *J. Magn. Magn. Mater.*, 2016, **420**, 309–316.

12 G. A. Petrakovskiĭ, L. N. Bezmaternykh, D. A. Velikanov, A. M. Vorotynov, O. A. Bayukov and M. Schneider, Magnetic properties of single crystals of ludwigites Cu_2MBO_5 (M = Fe^{3+}, Ga^{3+}), *Phys. Solid State*, 2009, **51**(10), 2077–2083.

13 L. N. Bezmaternykh, E. M. Kolesnikova, E. V. Eremin, S. N. Sofronova, N. V. Volkov and M. S. Molokeev, Magnetization pole reversal of ferromagnetic ludwigites $Mn_{3-x}Ni_xBO_5$, *J. Magn. Magn. Mater.*, 2014, **364**, 55–59.

14 E. Moshkina, S. Sofronova, A. Veligzhanin, M. Molokeev, I. Nazarenko, E. Eremin and L. Bezmaternykh, Magnetism and structure of Ni_2MnBO_5ludwigite, *J. Magn. Magn. Mater.*, 2016, **402**, 69–75.

15 S. Sofronova, E. Moshkina, I. Nazarenko, A. Veligzhanin, M. Molokeev, E. Eremin and L. Bezmaternykh, Chemical disorder reinforces magnetic order in ludwigite $(Ni,Mn)_3BO_5$ with Mn^{4+} inclusion, *J. Magn. Magn. Mater.*, 2018, **465**, 201–210.

16 L. Bezmaternykh, E. Moshkina, E. Eremin, M. Molokeev, N. Volkov and Y. Seryotkin, Spin-lattice coupling and peculiarities of magnetic behavior of ferrimagnetic ludwigites $Mn^{2+}_{0.5}M^{2+}_{1.5}Mn^{3+}BO_5$ (M=Cu, Ni), *Solid State Phenom.*, 2015, **233–234**, 133–136.

17 D. V. Popov, T. P. Gavrilova, I. F. Gilmutdinov, M. A. Cherosov, V. A. Shustov, E. M. Moshkina, L. N. Bezmaternykh and R. M. Eremina, Magnetic properties of ludwigite $Mn_{2.25}Co_{0.75}BO_5$, *J. Phys. Chem. Solids*, 2021, **148**, 10969.

18 L. N. Bezmaternykh, S. N. Sofronova, N. V. Volkov, E. V. Eremin, O. A. Bayukov, I. I. Nazarenko and D. A. Velikanov, Magnetic properties of $Ni_3B_2O_6$ and $Co_3B_2O_6$ single crystals, *Phys. Status Solidi B*, 2012, **249**(8), 1628–1633.

19 N. A. Toropov, V. P. Barzakovskiy, V. V. Lapin and N. N. Kurtseva, *Status diagrams of silicale systems*, Nauka, Moscow (Russia), 1969, pp. 1–822.

20 A. G. Gamzatov, Y. S. Koshkid'ko, D. C. Freitas, E. Moshkina, L. Bezmaternykh, A. M. Aliev, S.-C. Yu and M. H. Phan, Anisotropic magnetocaloric properties of theludwigite single crystal Cu2MnBO5, *Appl. Phys. Lett.*, 2020, **116**, 232403.

21 A. A. Dubrovsky, M. V. Rautskii, E. M. Moshkina, I. V. Yatsyk and R. M. Eremina, EPR-DeterminedAnisotropyofthe g-Factor and Magnetostriction of a Cu_2MnBO_5 Single Crystal with a Ludwigite Structure, *JETP Lett.*, 2017, **106**, 716–719.

22 G. M. Sheldrick, *Acta Crystallogr., Sect. A: Found. Crystallogr.*, 2008, **64**, 112–122.

23 *PLATON – A Multipurpose Crystallographic Tool*, Utrecht University, Utrecht, The Netherlands, 2008.
24 K. Brandenburg and M. Berndt, *DIAMOND - Visual Crystal Structure Information System CRYSTAL IMPACT*, Postfach 1251, D-53002 Bonn.
25 E. Moshkina, Y. Seryotkin, A. Bovina, M. Molokeev, E. Eremin, N. Belskaya and L. Bezmaternykh, Crystal formation of Cu-Mn-containing oxides and oxyborates in bismuth-boron fluxes diluted by MoO_3 and Na_2CO_3, *J. Cryst. Growth*, 2018, **503**, 1–8.
26 S. Sofronova and I. Nazarenko, Ludwigites: From natural mineral to modern solid solutions, *Cryst. Res. Technol.*, 2017, **52**(4), 1600338.
27 K. Bluhm and Hk. Muller-Buschbaum, Zur Stabilisierung der Oxidationsstufe M^{IV} im $Ni_5MB_2O_{10}$ – Typ, *Z. Anorg. Allg. Chem.*, 1989, **579**, 111–115.
28 C. A. F. Leite, R. B. Guimaraes, J. C. Fernandes, M. A. Continentino, C. W. A. Paschoal, A. P. Ayala and I. Guedes, Temperature-dependent Raman scattering study of $Fe_3O_2BO_3$ ludwigite, *J. Raman Spectrosc.*, 2001, **33**, 1–5.
29 J. Manzi, A. Paolone, O. Palumbo, D. Corona, A. Massaro, R. Cavaliere, A. B. Muñoz-García, F. Trequattrini, M. Pavone and S. Brutti, Monoclinic and Orthorhombic $NaMnO_2$ for Secondary Batteries: A Comparative Study, *Energies*, 2021, **14**, 1230.
30 X. Zhu, F. Meng, Q. Zhang, L. Xue, H. Zhu, S. Lan, Q. Liu, J. Zhao, Y. Zhuang, Q. Guo, B. Liu, L. Gu, X. Lu, Y. Ren and H. Xia, $LiMnO_2$ cathode stabilized by interfacial orbital ordering for sustainable lithium-ion batteries, *Nat. Sustain.*, 2021, **4**, 392–401.
31 P. Vassilaras, X. Ma, X. Li and G. Ceder, Electrochemical Properties of Monoclinic $NaNiO_2$, *J. Electrochem. Soc.*, 2013, **160**(2), A207–A211.
32 L. D. Dyer, B. S. Borie Jr and G. P. Smit, Alkali Metal-Nickel Oxides of the Type $MNiO_2$, *J. Am. Chem. Soc.*, 1954, **76**(6), 1499–1503.